Available online at www.sciencedirect.com
ScienceDirect
Journal of Pharmaceutical and Biomedical Analysis 43 (2007) 1595–1601
JOURNAL OF PHARMACEUTICAL AND BIOMEDICAL ANALYSIS
www.elsevier.com/locate/jpba

^{1}H and ^{19}F NMR relaxation studies of fleroxacin with *Micrococcus luteus*

Benjamin Waibel, Ulrike Holzgrabe *

Institute of Pharmacy and Food Chemistry, University of Würzburg, Am Hubland, 97074 Würzburg, Germany

Received 26 June 2006; received in revised form 7 December 2006; accepted 24 December 2006
Available online 23 January 2007

Abstract

In order to investigate and characterize interaction processes between the fluoroquinolone fleroxacin and bacterial cells we used non-selective (all resonances are excited), selective (observed resonance is excited) spin–lattice relaxation rates and spin–spin relaxation measurements. The signals of three hydrogens at different moieties of the fleroxacin molecule were considered to get an insight in the complexation behavior. The enhancement of selective relaxation rates was observed with increasing fleroxacin concentrations and keeping the bacterial mass constant. The obtained relaxation rates of the affected hydrogens were analyzed via a Lineweaver–Burk-plot to determine the K_D values. Furthermore, ^{19}F NMR spectra were recorded and spin–spin relaxation rates (R_2) were determined by a Carr–Purcell–Meiboom–Gill (CPMG) pulse sequence. Because of the dependency of the line width of NMR peaks on transversal relaxation time T_2, we compared the line width at half-height at different fleroxacin concentrations in order to investigate the involvement of fluorine atoms in different positions in the complexation. All findings point to core quinolone moiety to be involved in the interaction with bacterial cells.

Keywords: NMR; Fluoroquinolone; Bacteria; ^{1}H spin–lattice relaxation rate; ^{19}F spin–spin relaxation rate; Dissociation constant

1. Introduction

Fluoroquinolones are an important tool in the therapy of many bacterial infections, e.g. of the respiratory tract or urinary tract [1,2]. They have a wide spectrum of activity against both Gram-positive and Gram-negative pathogens. The quinolones are inhibitors of the bacterial type II topoisomerase, called gyrase. This enzyme is localized inside the bacteria cell and is responsible for the introduction of negative supercoils into the DNA [3]. The detailed mechanism of the interaction of quinolones with the gyrase and the DNA building a ternary complex is not yet fully understood because neither an X-ray nor a NMR-structure could be solved [4].

As the target of the fluoroquinolones is intracellular, they have to cross the inner and outer membrane of the bacterial cell wall [5]. Two mechanisms are known: hydrophobic quinolones such as nalidixic acid diffuse through the bacterial bilayer membrane passively whereas the hydrophilic group, e.g. ofloxacin and ciprofloxacin, is transported by transmembrane porin proteins [6–9]. The latter hypothesis was proofed by knocking out a specific porin *ompF*, which results in a low concentration of the anti-infective agent in the bacterial cell [10]. Fleroxacin belongs to the fluoroquinolones who seems to penetrate via the porin transport protein *ompF* [11].

In order to examine the effect of antibiotics to bacterial systems spectroscopic analysis, such as IR absorption and Raman spectroscopy, can be applied [12]. NMR spectroscopy has been shown to be a screening technique, which can be used to observe interactions of small molecules (i.e. ligands) with macromolecules (i.e. receptors and enzymes) in case of fast exchange between the free and the bound state [13]. Various methods such as chemical shift differences [14–16], line width analysis, relaxation measurements, determination of diffusion coefficients [17] and intermolecular magnetization transfer techniques such as tr-NOE [18,19] or WaterLOGSY experiments [20] have been reported. There are a number of studies based on relaxation measurements for determination of ligand–macromolecule binding [21–26]. Both longitudinal (T_1) and transverse (T_2) relaxation times are dependent on the dipolar interaction between a macromolecule and a substrate. The ligand must, however, be in fast exchange between the free and the bound states to constitute the ligand as a binder. Most NMR investigations performed in various binding studies consist of the selective ($R_{1,s}$) and non-selective ($R_{1,ns}$) spin–lattice relaxation rates of the ligand with

* Corresponding author. Tel.: +49 9318885461; fax: +49 9318885494.
E-mail address: holzgrab@pharmazie.uni-wuerzburg.de (U. Holzgrabe).

0731-7085/$ – see front matter © 2007 Elsevier B.V. All rights reserved.
doi:10.1016/j.jpba.2006.12.018

and without a macromolecule, which might represent the bacterial cell wall, an enzyme inside the bacterium or other proteins [27]. Thereby, the formed ligand–macromolecule complex can affect the relaxation times of the hydrogen's resonance of the ligand in different ways. However, measuring non-selective $T_{1,ns}$, where all resonances in the spectrum are excited, the relaxation rates do not show a direct dependence on the mobility of the molecule characterized by the correlation time and thus, cannot be used for screening purposes.

Since gyrase inhibitors of the quinolone-type interact with various macromolecules of the bacterial cell, e.g. in the quinolone–gyrase–DNA complex, with porines of the cell membrane and with the outer cell membrane, and none of these interactions could be characterized till now, we decided to study the interaction of the quinolones with whole bacterial cells by means of NMR spectroscopy. This approach has the advantage to be close to *in vivo* conditions. However, we are aware of the fact that it will be difficult to find out which macromolecule of the bacterial cell will be complexed. To the best of our knowledge no such study with antibiotics and whole bacterial cells has been performed till now.

Preliminary measurements of the diffusion coefficient (D) of ofloxacin in presence and in absence of *Micrococcus luteus* provided a first indication of binding to a macromolecule due to the decreased D value (B. Waibel, R. Deubner, U. Holzgrabe, unpublished results). Beside the change of the diffusion constant of the antibiotic, the D of the water also decreased by the addition of the bacterial cells. Since the diffusion measurements are very sensitive to viscosity variations of the solution and temperature effects the results are to some extent uncertain. Beside the change of the diffusion coefficient by the binding to the cell, D will be additionally affected by the descent of the cells in the NMR tube. Thus, the determination of K_D via D is hard to analyze.

Therefore, we decided to study the interaction of quinolones with whole bacterial cells by means of ^{1}H NMR selective spin–lattice and ^{19}F spin–spin relaxation measurements. Both methods offer a possibility to examine the mode of complexation with macromolecules and can also offer evidence which substructure of fleroxacin is highly involved in this binding. Fleroxacin was chosen because of its three fluorine atoms, arranged on different important molecular substructures. By ^{19}F measurements these substructures could be investigated closer and thus we could get a clue of the binding behavior for every part of the molecule. Measuring the ^{19}F NMR spectra can provide enormous advantages versus ^{1}H measurements. Remaining water in the sample may disturb ^{1}H measurements to a high extend since the receiver gain of the spectrometer has to be decreased due to the strong water signal and therefore small signals of the ligand can be disturbed. Furthermore, as the bacterial macromolecules do not contain fluorine we do not expect signals of the cells disturbing the exact analysis of some antibiotic signals.

Even if we do not exactly know the macromolecule, which is involved in the binding of fleroxacin in a complete biological system, we were able to prove that there exists a specific binding, indicated by a defined K_D value.

2. Materials and methods

2.1. Materials

Fleroxacin, kindly donated by F. Hoffmann-La Roche Ltd. (Basel, Switzerland), was used to produce a stock solution of 50 mM. For this purpose 55.4 mg of fleroxacin were suspended in 3 mL D_2O and 15 μL of NaOD 39.9% in D_2O. D_2O was purchased from Euriso-Top (Gif-sur-Yvette, France), NaOD 39.9% from Deutero GmbH (Kastellaun, Germany). Fleroxacin was completely dissolved by ultra-sonication for 30 min.

Phosphate-buffered saline (PBS) consisted of 22.19 mM Na_2HPO_4, 5.31 mM NaH_2PO_4, 100 mM NaCl (of a pH of 7.4) and was dissolved in deuteriumoxide. All solutions were degassed by ultra-sonication for 30 min before use.

2.2. Bacteria

Micrococcus luteus was obtained from DSZM (Braunschweig, Germany) as a vacuum-dried culture, which was cultivated on Mueller–Hinton agar (beef, dehydrated infusion of 300 g, 2 g/L; casein hydrolysate, 17.5 g/L; starch, 1.5 g/L) from Oxoid (Wesel, Germany). The bacterial amount needed was directly harvested from the culture plate and suspended in 50 mM PBS in deuteriumoxide. The suspension was pelleted by ultracentrifugation at 3400 rpm for 5 min, using a centrifuge (ETA 12; Hettich, Kirchlengern, Germany). The supernatant was discarded and the pellet was washed three times with D_2O–PBS to remove the culture media components. The cells were suspended in D_2O–PBS and the corresponding amount of the antibiotic stock solution was added. In all measurements 50.0 mg bacterial mass were applied corresponding to $\sim 2.0 \times 10^{10}$ cells/mL determined via optical density (OD) measurements at 600 nm at an UV/Vis Shimadzu (Kyoto, Japan) spectrometer.

The viability of *M. luteus* after an experiment without fleroxacin was determined by a fluorescence assay using the BacLight kit of Invitrogen (Karlsruhe, Germany), containing two different stains—SYTO 9 and propidium iodide. Because of the different cell membrane integrity for the two stains, intact cells appear green (SYTO 9) while non-intact cells appear red (propidium iodide). The amount of living cells was analyzed by a regression analysis with different ratios of living and dead cells, killed by suspension in 70% isopropanol for 4 h. After the NMR relaxation experiments, the viability of the bacteria was determined and found to be 73%.

2.3. NMR spectroscopy

All measurements were performed on a Bruker Avance 400 FT NMR spectrometer (Bruker, Rheinstetten, Germany) operating at 400.13 MHz for ^{1}H and 376.43 MHz for ^{19}F. All experiments were carried out at a temperature of 310 K. ^{1}H spectra were recorded using a BBO broadband probe. 16 scans were collected into 32k data points giving a digital resolution of 0.24 Hz/point at a spectral width of 4006 Hz. A selective ^{19}F probe (SEF) was applied for ^{19}F NMR spectra. 16 scans were

measured into 128k data points giving a digital resolution of 0.14 Hz/point at a spectral width of 9057 Hz. To evaluate the data and to calculate relaxation times we used the XWIN-NMR program package version 3.5 of Bruker (Rheinstetten, Germany) running on a Microsoft Windows PC.

Non-selective spin–lattice relaxation rates were measured using a 180°-τ-90°-inversion recovery experiment. The τ-values used for the selective and non-selective experiments were: 0.01, 0.1, 0.25, 0.5, 1, 2, 3, 6, 10, 15 s. Relaxation times were calculated by exponential regression analysis of recovery curves of longitudinal magnetization components. Thereby an area fit of the respective peaks was performed.

Developing a selective 180° pulse to determine selective spin–lattice relaxation rates we used a Gauss 1.100 soft pulse with a length of 47 msec and a power of 60 dB corresponding to an excitation width of about 45 Hz.

Spin–spin ^{19}F-relaxation times were defined by using a Carr–Purcell–Meiboom–Gill (CPMG) pulse sequence [28]. A non-selective 90° pulse of 12.1 μs was used to excite the sample and multiple, non-selective 180° refocusing pulses of 24.1 μs generated the echo train. The time between the 180° pulses, τ_{cp}, was 2.5 ms. τ_{cp} was $\ll 1/J^{F,H}$ to minimize scalar coupling ($J^{F,H}$) evolution. 2, 4, 6, 12, 18, 24, 32, 58, 100, 150 loops were used during all CPMG sequences. In all relaxation measurements, the time between two sequences (d_1) was chosen to 20 s, which is always higher than five times T_1 to ensure the complete relaxation of the system.

3. Results and discussion

3.1. Non-selective and selective T1 ^{1}H-measurements of fleroxacin

In order to observe a ligand binding to a macromolecule, the ligand must have a moderate to fast exchange between free and bound state in average. Slow exchange binders will appear as non-binding molecules. In case of fast exchange the observed relaxation rate $R_{1,obs}$ is given by the equation [13,24]:

$$R_{1,obs} = fR_{1,bound} + (1 - f)R_{1,free} \quad (1)$$

where f is the fraction of the bound ligand and $R_{1,bound}$ and $R_{1,free}$ are the longitudinal relaxation rates for the bound and free states.

There are two possibilities to perform a longitudinal relaxation measurement. On the one hand, all resonances can be excited simultaneously applying a non-selective 180° pulse and on the other hand, by inverting a single signal in performing a selective pulse. The non-selective ($R_{1,ns}$) and the selective relaxation rate ($R_{1,s}$) of a proton i for a dipole–dipole interaction with another proton j are given by [13]:

$$R^i_{1,ns} = \sum_{j \neq i} \frac{\gamma^4 \hbar^2}{10 r^6_{ij}} \left\{ \frac{3\tau_c}{1 + \omega^2_H \tau^2_c} + \frac{12\tau_c}{1 + 4\omega^2_H \tau^2_c} \right\} \quad (2)$$

$$R^i_{1s} = \sum_{j \neq i} \frac{\gamma^4 \hbar^2}{10 r^6_{ij}} \left\{ \frac{3\tau_c}{1 + \omega^2_H \tau^2_c} + \frac{6\tau_c}{1 + 4\omega^2_H \tau^2_c} + \tau_c \right\} \quad (3)$$

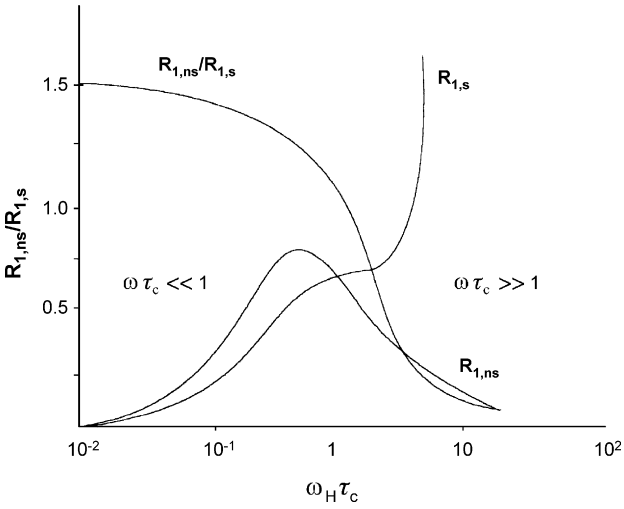

Fig. 1. Plot of $R_{1,ns}$, $R_{1,s}$ and the $R_{1,ns}/R_{1,s}$ ratio as a function of ω_H τ_c for glycyl-L-tyrosine bound to carboxypeptidase A modified from Valensin et al. [29].

where $\hbar$ is the reduced Planck constant, γ is the ^{1}H gyromagnetic ratio, ω_H is the proton Larmor frequency, τ_c is the correlation time and r_{ij} is the intermolecular distance between proton i and proton j. $R_{1,s}$ is directly dependent on τ_c which results in the plot shown in Fig. 1 [29]. Both relaxation rates are displayed as a function of the correlation time. Only $R_{1,s}$ can be used as a screening technique for binding behaviour of small molecules to macromolecules because of the lack of the τ_c dependence on the non-selective relaxation rates. A Lineweaver–Burk-type plot allows to extrapolate the K_D by plotting the ligand concentration [L_{tot}] versus the reciprocal difference between the observed $R_{1,s}$ in presence and absence of the bacteria ($1/\Delta R_{1,s}$). At $1/\Delta R_{1,s} = 0$ the [L_{tot}] value corresponds to the negative K_D [30].

The ^{1}H assignment of the hydrogens of fleroxacin is displayed in Fig. 2. An example of the selective excitation of a signal is shown in Fig. 3. By means of the determination of selective and non-selective relaxation rates of three significant hydrogens, we wanted to get an insight in the binding involvement of each substructure of fleroxacin (pyridone-, piperazine- and aromatic-moiety). For this purpose H2, H5 and the N-methyl group were selectively excited and the longitudinal relaxation times were measured. Relaxation data for fleroxacin in presence and absence of *M. luteus* are displayed in Table 1. The hydrogens (H_a, H_b) of the piperazine ring and of the fluoroethylene group were hard to analyze because of the broad bacterial ^{1}H resonances lying in the same chemical shift region (Fig. 2) and therefore disturb the correct determination of the hydrogen relaxation rates. Fig. 4 showing a comparison of $R_{1,ns}$ and $R_{1,s}$ of H2 demonstrates that the non-selective relaxation rates are almost not influenced by increasing fleroxacin concentrations. In turn, the selective spin–lattice relaxation rates $R_{1,s}$ showed a direct dependence on τ_c. This is consistent with the aforementioned theory that only selective measurements can serve as a screening technique in exploring interaction processes.

In order to determine the dissociation constants for fleroxacin, $\Delta R_{1,s}$ values were measured in presence of increasing

Table 1
Non-selective ($R_{1,ns}$) and selective ($R_{1,s}$) spin–lattice relaxation rates of fleroxacin (10 mM) in presence (+) and absence (−) of *Micrococcus luteus* (2.0×10^{10} cells/mL)

	H2			H5			N-CH_3		
	$R_{1,ns}$ (s^{-1})	$R_{1,s}$ (s^{-1})	$R_{1,ns}/R_{1,s}$	$R_{1,ns}$ (s^{-1})	$R_{1,s}$ (s^{-1})	$R_{1,ns}/R_{1,s}$	$R_{1,ns}$ (s^{-1})	$R_{1,s}$ (s^{-1})	$R_{1,ns}/R_{1,s}$
−*M. luteus*	0.7692	0.7215	1.0662	0.5974	0.5491	1.0879	1.4144	1.595	0.88677
+*M. luteus*	0.9066	1.3665	0.6634	0.5420	0.9960	0.5442	1.5146	1.7714	0.8550

ligand concentrations at a fixed bacterial concentration. Due to the binding to a macromolecule, e.g. the bacterial cell wall or proteins, and thus developing dipole–dipole interactions the relaxation rates enhances with increasing ligand concentration. A Lineweaver–Burk plot of the titration of fleroxacin is displayed in Fig. 5 for each affected protons and K_D values were extrapolated to $\Delta R_{1,s} = 0$. K_D values obtained for the hydrogens at the quinoline structure H2 and H5 are 3.6127 mM and 3.3171 mM, respectively, indicating that the entire quinolone substructure is involved in the binding to the macromolecule. The K_D determination of the N-methyl group of the piperazinyl group resulted in relaxation times between 562 (5 mM) and

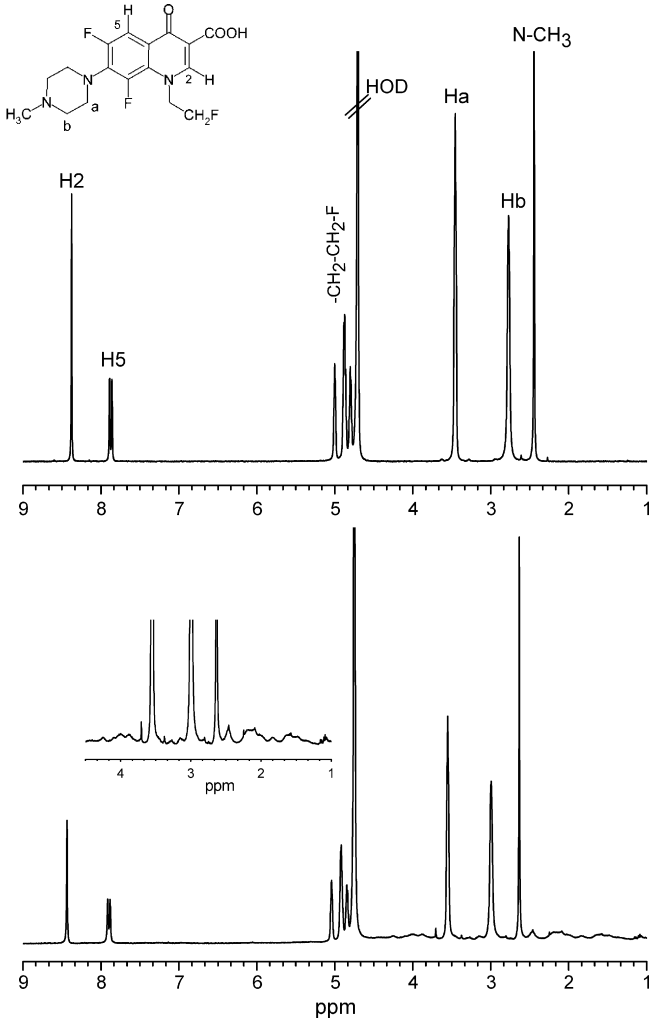

Fig. 2. ^{1}H spectrum and structure of fleroxacin 10 mM in D_2O–PBS (top) and ^{1}H spectrum of fleroxacin 10 mM in presence of 2.0×10^{10} cells/mL *M. luteus* (lower) measured each at 400 MHz and 310 K using 16 scans.

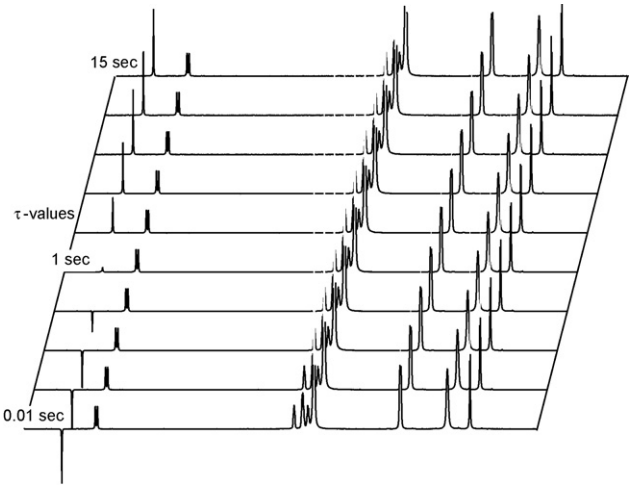

Fig. 3. Stacked plot of the selective relaxation measurement of H2 with τ-values of 0.01, 0.1, 0.25, 0.5, 1, 2, 3, 6, 10, 15 s.

572 ms (30 mM) making an exact measurement of K_D difficult. However, the approximate K_D of 98.776 mM alludes to the fact that the piperazine ring is not bound to the macromolecule. After the NMR experiments, 73% of the bacterial cells were still alive demonstrating that the binding is not a matter of unspecific binding to cell fragments of lysed bacteria.

3.2. ^{19}F spin–spin relaxation measurements of fleroxacin

In fast exchange between ligand and macromolecule the observed transverse relaxation rates R_2 is defined by the

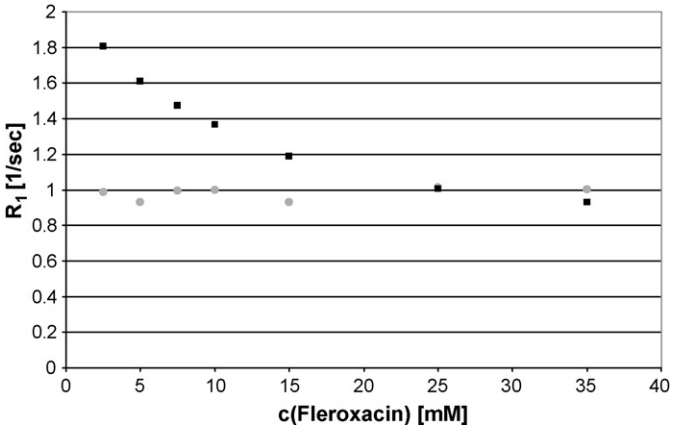

Fig. 4. Selective (■) and non-selective (●) relaxation rates of H2 vs. fleroxacin concentration in presence of 2.0×10^{10} cells/mL.

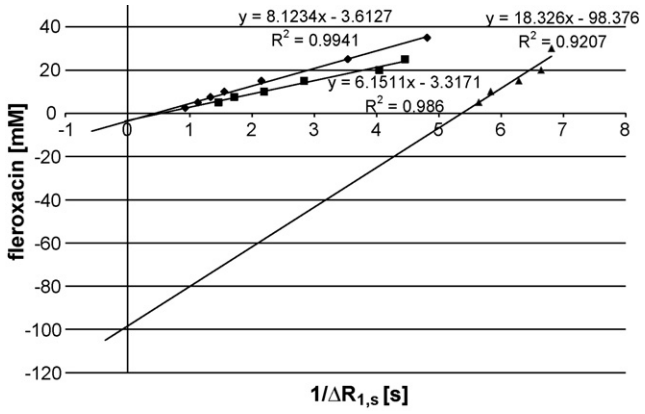

Fig. 5. Lineweaver–Burk plot of H2 (♦), H5 (■) and N-CH_3 (▲) hydrogens in D_2O–PBS at 310 K in presence of 2.0×10^{10} cells/mL.

equation [13]:

$$R_{2,\mathrm{obs}} = fR_{2,\mathrm{bound}} + (1-f)R_{2,\mathrm{free}} + f(1-f)^2 \frac{4\pi^2(\delta_{\mathrm{free}} - \delta_{\mathrm{bound}})^2}{K_{-1}} \quad (4)$$

where $R_{2,\mathrm{bound}}$ and $R_{2,\mathrm{free}}$ are the spin–spin relaxation rates for the ligand in bound and free states. δ_{bound} and δ_{free} are the chemical shifts for the observed resonance in bound and free states. K_{-1} is the residence time of the bounded ligand. The last term can be neglected in fast exchange.

In terms of spectral densities R_2 can be approximately described by:

$$R_2^i = \sum_{j \neq i} \frac{\gamma^4 \hbar^2}{10 r_{ij}^6} \left\{ \frac{15\tau_c}{2(1+\omega_H^2\tau_c^2)} + \frac{3\tau_c}{1+4\omega_H^2\tau_c^2} + \frac{9}{2}\tau_c \right\} \quad (5)$$

Due to the direct dependence of R_2 to τ_c (as already described for the selective spin–lattice relaxation rates $R_{1,s}$), the transverse relaxation rates can also be consulted for screening purposes.

A binding of a ligand can also be seen by the line broadening of the signal because the linewidth is equal to R_2/π. A fast insight in the binding mode of the ligand can be correspondingly obtained by comparing the signal line widths at half-height (HLW).

As already mentioned, fluorine NMR can be advantageous to the ^{1}H NMR spectroscopy. In principle, the bacterial suspension could be directly measured in the culture medium with an addition of D_2O to ensure the lock. Thus, the long washing procedures of the bacterial sample could be dropped. Also, the broad signals of the bacterial cells do not emerge in the spectrum, which is a very adjuvant fact to evaluate transverse relaxation rates correctly. A ^{19}F spectrum of fleroxacin is displayed in Fig. 6. All resonances were analysed with respect to their transverse relaxation rates and peak width at half-height (Table 2). Both R_2 and HLW are showing almost the same results. Due to the stronger line broadening and the stronger effect of the relaxation rate, the fluorine at position 6 seems to be more affected by the binding to the macromolecule than the fluorine at position 8. The signal of fluorine attached to the N_1-ethylene group is almost not influenced. A comparison of HLW and R_2 of the three fleroxacin fluorine resonances is displayed in Fig. 7. The observations made in the ^{19}F relaxation experiments lead to the assumption that the part of the aromatic moiety, enclosing C3 to C6, seems to be more involved in the binding than the fluorine position 8 next to the piperazine ring-system. The ethylene group is unaffected by the complexation and showed almost no change in relaxation rates due to the retained mobility of the unbound side chain.

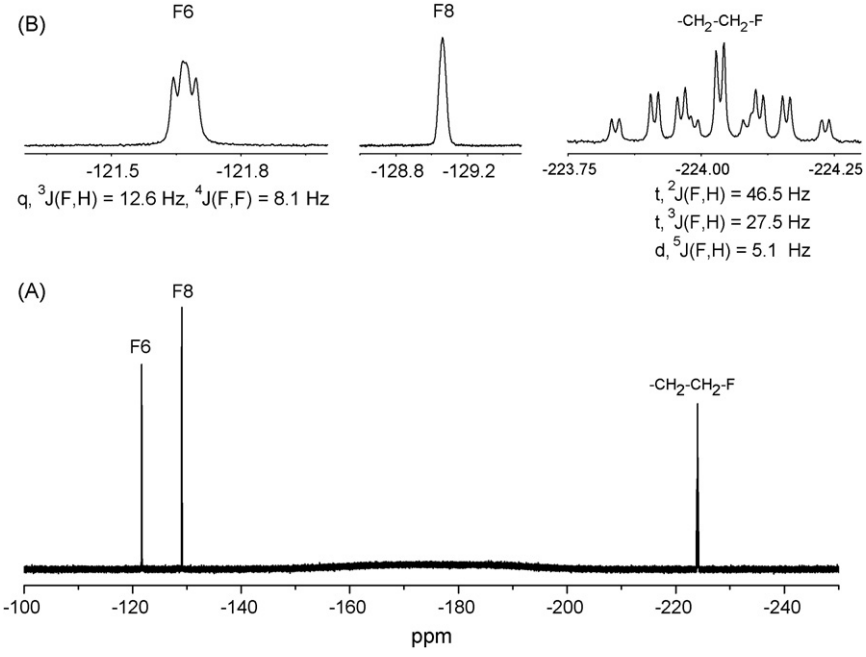

Fig. 6. ^{19}F spectrum of fleroxacin in D_2O–PBS recorded at 376 MHz with 16 scans. The entire spectrum (A) and expansions of the signals (B).

Table 2
Width of ^{19}F resonances at half width (HLW) and transverse relaxation rates (R_2) in dependence on the fleroxacin concentration in presence of 2.0×10^{10} cells *Micrococcus luteus*

Fleroxacin concentration (mM)	F6		F8		CH_2CH_2–F	
	HLW (Hz)	R_2 (s^{-1})	HLW (Hz)	R_2 (s^{-1})	HLW (Hz)	R_2 (s^{-1})
5	25.26	81.204	18.73	30.340	10.35	11.979
10	24.54	52.208	18.22	24.922	10.33	10.422
15	24.1	35.413	18.16	22.336	10.24	9.985
20	23.43	22.846	17.87	18.159	10.1	8.897
25	22.82	17.568	17.7	17.729	9.95	8.789
30	21.9	14.071	17.6	16.631	9.98	8.372

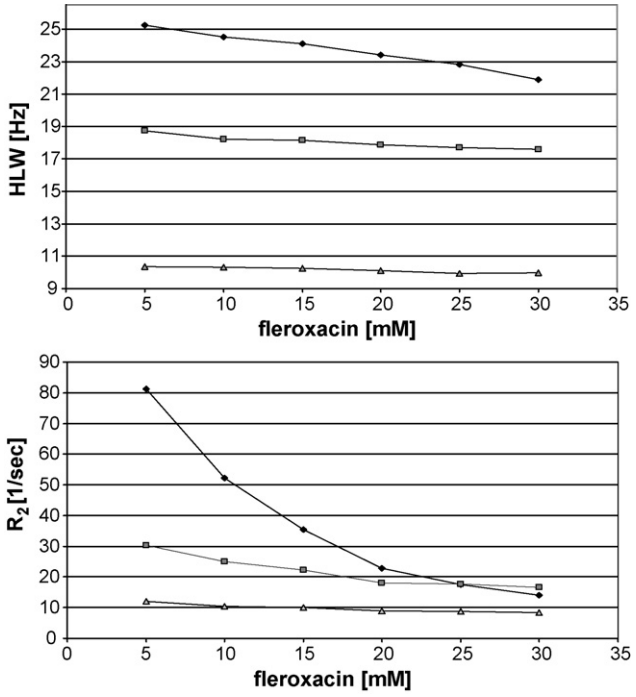

Fig. 7. Dependency of fleroxacin concentration on line width at half-height (above) and transversal relaxation rates (below) of F6 (♦), F8 (■) and CH_2CH_2–F (▲).

4. Conclusion

Determining non-selective and selective proton relaxation rates offered a very powerful tool to analyze and to get an access in the binding behaviour of a fluoroquinolone to a macromolecule. Determination of diffusion constants seems to be an additional method of choice to estimate the binding ability of fluoroquinolones to macromolecules. Due to the potential viscosity enhancement by the bacterial cells and the descent of the cells, conclusions from the diffusion data have to be handled with care. In these studies, NMR relaxation measurements have proved to be a very suitable method to estimate complexation behaviour of a ligand towards bacteria. Thereby, the performance of liquid NMR measurements in a bacterial cell suspension and the associated broad signals of the bacterial resonances did not interfere with the exact determination of the ligand relaxation rates. In the case of fleroxacin it could be shown that the quinolone binds only with the isoquinoline moiety to the macromolecule. The piperazine and the fluoroethylene group showed almost no effect upon complexation. The K_D value of fleroxacin could be determined by two different protons of the isoquinoline system. Consequently, both hydrogens belonging to the isoquinoline moiety yielded almost the same dissociation constant of about 3.5 mM showing the good reliability of this method. ^{19}F relaxation measurements further support the involvement of the isoquinoline substructures because F6 and F8 seem to be more influenced than the fluorine at the N_1-ethyl group.

However, even though we observed a defined binding behaviour characteristic for a specific interaction with a macromolecule, we cannot define the location of the binding, the bacterial cell wall, the porin-transport protein or the target protein, the gyrase. This has to be studied by using the potential isolated binding partners. Since the fluoroquinolones bind to a DNA-gyrase complex which additionally contains Mg^{2+} ions, this is a difficult task as has been shown by Lecomte et al. who did not succeed to characterize the ternary complex [31].

However, this study was able to show the possibilities of NMR to measure dissociation constants even in a whole bacterial cell system.

References

[1] E. Pestova, J.J. Millichap, G.A. Noskin, L.R. Peterson, J. Antimicrob. Chemother. 45 (2000) 583–590.
[2] R. Quintiliani, R.C. Owens, E.M. Grant, Infect. Dis. Clin. Pract. 8 (Suppl. 1) (1999) 28–41.
[3] T. Skauge, I. Turel, E. Sletten, Inorg. Chim. Acta 339 (2002) 239–247.
[4] K. Drlica, X. Zhao, Microbiol. Mol. Biol. Rev. 61 (1997) 377–392.
[5] L.J.V. Piddock, J. Antimicrob. Chemother. 27 (1991) 399–403.
[6] L.J.V. Piddock, Y.F. Jin, V. Ricci, A.E. Asuquo, J. Antimicrob. Chemother. 43 (1999) 61–70.
[7] K. Hirai, H. Aoyama, T. Irikura, S. Iyobe, S. Mitsuhashi, Antimicrob. Agents Chemother. 29 (1986) 535–538.
[8] J. Chevalier, M. Malléa, J.M. Pagès, Biochem. J. 348 (2000) 223–227.
[9] J. Bedard, S. Wong, L.E. Bryan, Antimicrob. Agents Chemother. 31 (1987) 1348–1354.
[10] P.G.S. Mortimer, L.J.V. Piddock, J. Antimicrob. Chemother. 32 (1993) 195–213.
[11] P. Rohner, M. Peebo, D.P. Lew, R. Auckenthaler, J.C. Pechère, J. Antimicob. Chemother. 29 (1992) 41–48.
[12] U. Neugebauer, U. Schmid, K. Baumann, U. Holzgrabe, W. Ziebuhr, S. Kozitskaya, W. Kiefer, M. Schmitt, J. Popp, Biopolymers 82 (2006) 306–311.
[13] B.J. Stockman, C. Dalvit, Progr. Nucl. Magn. Reson. Spectrosc. 41 (2002) 187–231.

[14] M.P. Foster, D.S. Wuttke, K.R. Clemens, W. Jahnke, I. Radhakrishnan, L. Tennant, M. Reymond, J. Chung, P.E. Wright, J. Biomol. NMR 12 (1998) 51–71.
[15] Y. Li, Q. Li, M. Sun, G. Song, S. Jiang, D. Zhu, Bioorg. Med. Chem. Lett. 14 (2004) 1585–1588.
[16] F. Bernardi, E. Gaggelli, E. Molteni, E. Porciatti, D. Valensin, Biophys. J. 90 (2006) 1350–1361.
[17] T. Brand, E.J. Cabrita, S. Berger, Prog. Nucl. Magn. Reson. Spectrosc. 46 (2005) 159–196.
[18] B. Meyer, T. Weimar, T. Peters, Eur. J. Biochem. 246 (1997) 705–709.
[19] J. Angulo, B. Langpap, A. Blume, T. Biet, B. Meyer, N.R. Krishna, H. Peters, M.M. Palcic, T. Peters, J. Amer. Chem. Soc. 128 (2006) 13529–13538.
[20] C. Dalvit, G.P. Fogliatto, A. Stewart, M. Veronesi, B. Stockmann, J. Biomol. NMR 21 (2001) 349–359.
[21] E. Gaggelli, G. Valensin, T. Kushnir, G. Navon, Magn. Reson. Chem. 30 (1992) 461–465.
[22] C. Rossi, C. Bonechi, S. Martini, M. Ricci, G. Corbini, P. Corti, A. Donati, Magn. Reson. Chem. 39 (2001) 457–462.
[23] M. Delfini, R. Gianferri, V. Dubbini, C. Manetti, E. Gaggelli, G. Valensin, J. Magn. Reson. 144 (2000) 129–133.
[24] S. Martini, C. Bonechi, M. Casolaro, G. Corbini, C. Rossi, Biochem. Pharmacol. 71 (2006) 858–864.
[25] G. Corbini, S. Martini, C. Bonechi, M. Casolaro, P. Corti, C. Rossi, J. Pharm. Biomed. Anal. 40 (2006) 113–121.
[26] P.J. Hajduk, E.T. Olejniczak, S.W. Fesik, J. Amer. Chem. Soc. 119 (1997) 12257–12261.
[27] G. Veglia, M. Delfini, M.R. Del Giudice, E. Gaggelli, G. Valensin, J. Magn. Reson. 130 (1998) 281–286.
[28] S. Meiboom, D. Gill, Rev. Sci. Instrum. 29 (1958) 688–691.
[29] G. Valensin, T. Kushnir, G. Navon, J. Magn. Reson. 46 (1982) 23–29.
[30] G. Valensin, P.E. Valensin, E. Gaggelli, in: J.W. Jaroszewski, K. Schaumburg, H. Kofod (Eds.), NMR Spectroscopy in Drug Research, Munksgaard, Copenhagen, 1988.
[31] S. Lecomte, N.J. Moreau, M.T. Chenon, Int. J. Pharm. 164 (1998) 57–65.